frontiers in Materials

ORIGINAL RESEARCH
published: 27 September 2019
doi: 10.3389/fmats.2019.00234

Influence of Protonic Ionic Liquid on the Dispersion of Carbon Nanotube in PLA/EVA Blends and Blend Compatibilization

Elaine Cristina Lopes Pereira[1]*, *Maria Eduarda C. Fernandes da Silva*[1], *Ketly Pontes*[2] and *Bluma Guenther Soares*[1,2]*

[1] Centro de Tecnologia, Instituto de Macromoléculas, Universidade Federal Do Rio de Janeiro, Rio de Janeiro, Brazil,
[2] Departamento de Engenharia Metalúrgica e de Materiais, Centro de Tecnologia, Universidade Federal Do Rio de Janeiro, Rio de Janeiro, Brazil

In this work, immiscible poly(lactic acid) (PLA)/poly(ethylene vinyl acetate) (EVA) composites with 1 phr of multi-walled carbon nanotube (CNT) and different concentration of protonic—based imidazolium ionic liquid (mimbSO$_3$H·Cl) were prepared. The protonic ionic liquid (IL) was able to act as dispersing agent for CNT and as compatibilizing agent for the PLA/EVA blend. The multicomponent nanocomposites from the mixture of PLA and EVA containing CNT functionalized with ionic liquid, IL (CNT/ILSO$_3$H) were characterized by mechanical and dynamic–mechanical (DMA) tests, electrical conductivity analyses, differential scanning calorimetry (DSC), X-ray diffraction analysis and rheological measurements, as well as chromatographic gel permeation (GPC), and scanning electron microscopy (SEM). The non-covalent functionalization CNT resulted in composites with outstanding electrical and dielectric properties. The high dispersion of CNT promoted by the IL resulted in the formation of a physical networked structure, which was responsible for the higher electrical conductivity and higher melt viscosity. The crystallization process of PLA phase was improved with the presence of CNT/ILSO$_3$H. The degradation process during the transesterification reaction did not significantly affect the mechanical properties. The present work highlights the dual role of the IL as compatibilizing and dispersing agent and opens new perspectives for developing new conducting systems with low percolation threshold based on the good dispersion of CNT and the confinement of the filler within a phase of a multiphasic polymeric system.

Keywords: poly (lactic acid), ethylene-vinyl acetate copolymer, ionic liquid, carbon nanotube, conducting composite, electric conductivity

OPEN ACCESS

Edited by:
Andrea Dorigato,
University of Trento, Italy

Reviewed by:
Arup R. Bhattacharyya,
Indian Institute of Technology Bombay, India
Luca Fambri,
University of Trento, Italy
Rafael Guntzel Arenhart,
Federal University of Santa Catarina, Brazil

***Correspondence:**
Elaine Cristina Lopes Pereira
nanequimica@gmail.com
Bluma Guenther Soares
bluma@metalmat.ufrj.br

Specialty section:
This article was submitted to Polymeric and Composite Materials, a section of the journal Frontiers in Materials

Received: *16 April 2019*
Accepted: *09 September 2019*
Published: *27 September 2019*

Citation:
Lopes Pereira EC, da Silva MECF, Pontes K and Soares BG (2019) Influence of Protonic Ionic Liquid on the Dispersion of Carbon Nanotube in PLA/EVA Blends and Blend Compatibilization. Front. Mater. 6:234. doi: 10.3389/fmats.2019.00234

INTRODUCTION

Due to the widespread use of plastics in the packaging industry, there is a growing interest in the use of biodegradable polymers as a substitute for conventional polymers to reduce the environmental impact of plastic waste. Poly lactic acid (PLA) is a good example of these materials obtained from renewable resources (Lim et al., 2008; Nampoothiri et al., 2010). Besides being biodegradable and biocompatible, PLA also presents good processability when compared with other biodegradable polymers. However, it is quite rigid and brittle,

presents low moisture resistance and slow crystallization rate, which in turn limit its applications. Therefore, blending PLA with soft materials is a good strategy for overcoming these drawbacks. The appropriate choice of non-biodegradable polymers as component for PLA-based blends should reduce the biodegradation rate, cost and improve some mechanical properties. In these cases, the PLA phase undergoes a gradual degradation process, known as biodisintegration, resulting in very small pieces of the non-biodegradable polymer (Sarasa et al., 2009). A promising partner for blending with PLA is ethylene-vinyl acetate copolymer (EVA) due to its availability, low cost and versatility of applications, as it can present rubber or thermoplastic characteristics by changing the vinyl acetate (VA) content in the copolymer. Several papers have used EVA with different vinyl acetate content for the preparation of PLA/EVA blends for different purposes (Yoon et al., 1999; Li et al., 2011; Moura et al., 2011, 2012; Ma et al., 2012, 2015; Aghjeh et al., 2015, 2016; Sangeetha et al., 2016, 2018; Wang et al., 2016; Zhang and Lu, 2016; Lopes Pereira et al., 2017).

Blending conducting fillers as carbon nanotube (CNT) expands the field of applications of these semi-biodegradable composite as antistatic, dielectric and microwave absorbing materials for utilization in electronic packaging. Most of the studies involving CNT-based PLA/EVA composites focused on the improvement of mechanical properties and toughness of the blends (Shi et al., 2011, 2012; Wang et al., 2015, 2016; Liu et al., 2016). Studies related with the electrical properties of PLA/EVA blends loaded with CNT was reported by Shi et al. (2013). They used a master batch of PLA to prepare PLA/EVA (60:40 wt%) composites with different amounts of CNT. Resistivity values around 10^7 Ω·cm were obtained by adding 1 wt% of CNT. Higher amount of CNT did not affect the resistivity values.

A good distribution/dispersion of CNT within a thermoplastic matrix by melt mixing process is not an easy task due to the strong tendency to filler agglomeration caused by the highly conjugated structure and the Van der Waals interactions of CNT. To improve the dispersion of CNT in a polymer matrix, two strategies have been recently adopted: covalent and non-covalent surface functionalization. Covalent functionalization is based on chemical reactions on the surface of the CNT to introduce functional groups capable of reacting or interacting with the polymer matrix (Spitalsky et al., 2010). This methodology greatly facilitates the dispersion of CNT in polymer matrices, but destroys the π conjugation at the CNT surface, which is essential for good electrical conductivity. Therefore, the non-covalent functionalization is preferred because it does not destroy the conjugation at the CNT surface, besides being environmentally friendly because no chemical reactions with strong acids followed by purification are involved during the procedure. In this context, ionic liquid (IL) proved to be an excellent surface modifier for CNT since it efficiently interacts with the π cloud of the CNT, thus promoting a disaggregation of the CNT bundles and ropes (Fukushima et al., 2003).

Recently, several works in the literature reported the efficiency of the non-covalent functionalization of CNT with ILs to improve the dispersion of the filler within polymeric matrices consisted of epoxy resin (Lopes Pereira and Soares, 2016; Alves et al., 2018; Soares, 2018), thermoplastics (Zhao et al., 2012; Soares da Silva et al., 2017; Fang et al., 2018), elastomers (Subramaniam et al., 2013; Abraham et al., 2017; Hassouneh et al., 2017), as well as heterogeneous polymer blends (Bose et al., 2008; Soares et al., 2018; Lopes Pereira et al., 2019). Usually the presence of IL significantly increases the conductivity of the system.

Based on the importance of the theme for the electro-electronic, automobile and packaging industries, the aim of the present study is to investigate the efficiency of the protonic IL based on imidazolium cation as a dispersing agent for CNT in PLA/EVA blends and how the IL-CNT combination should affect the compatibility, morphology, electrical conductivity, mechanical and rheological properties. This protonic IL was recently reported as compatibilizing agent for PLA/EVA blends through a transesterification process (Lopes Pereira et al., 2017). To the best of our knowledge, no studies involving the functionalization of CNT with protonic IL and its use in polymer blends have been reported in the accessible literature. For this study, EVA containing 19 wt% of vinyl acetate (VA) was employed due to its great availability. PLA/EVA18 blend composition corresponding to 60:40 wt% was chosen for this study in order to increase the toughness of PLA while maintaining the biodegradability of the PLA matrix.

EXPERIMENTAL SECTION

Materials

Multiwalled CNT (pristine CNT–pCNT) (NC7000) was supplied by Nanocyl (Sambreville, Belgium) (average diameter = 59.5 nm; average length = 51.5 mm; surface area = 5,250–300 m^2/g). Ethylene vinyl acetate (EVA) copolymer with melt flow index = 2.5 g/10 min at 190°C/2.16 kg; vinyl acetate content = 19 wt%; density = 0.95 g/cm^3; melting temperature, Tm = 90°C and glass transition temperature, Tg = −14°C (Yamaki et al., 2002) was purchased from Braskem (São Paulo, Brazil). Poly (lactic acid) (PLA) designed for injection molding applications (trade name Ingeo™ Biopolymer 3251D; Mn = 80,000–90,000 $g{\cdot}mol^{-1}$; D isomer content = 4%; melt flow index = 35 g/10 min at 190°C/2.16 kg; density = 1.24 g/cm^3; glass transition temperature, Tg = 55–60°C; Tm = 155–170°C) was purchased by Nature Works LLC. N-methyl-imidazole and 1,4-butane sultone used for the synthesis of the protonic IL were supplied by Sigma-Aldrich.

Preparation of Sulfonic Acid–Based Ionic Liquid

The 1-methyl-imidazolium-3-butylsulfonic acid chloride [$mimbSO_3H{\cdot}Cl$] ionic liquid was synthesized by reacting N-methyl-imidazole and butane-sultone, followed by a treatment with hydrochloric acid, according to the literature (Lopes Pereira et al., 2017). The structure of the ionic liquid, $mimbSO_3H{\cdot}Cl$, is illustrated in **Figure 1** (yield = 75–85%; melting point = −59°C) and was confirmed by ^1H NMR spectrum (300 MHz, CDCl3) δ 1.85 (t, 2H), 2.17 (t, 2H), 3.05 (t, 2H), 4.05 (s, 3H), 4.4 (t,2H), 7.6 (d, 2H), 8.82 (s, 1H).

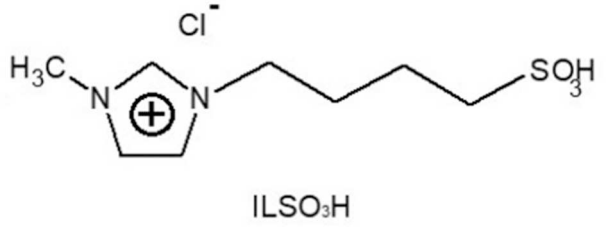

FIGURE 1 | Structure of the ionic liquid 1-methyl-imidazolium-3-butylsulfonic acid chloride [mimbSO$_3$H·Cl].

SAMPLE PREPARATION

The blend composition was fixed as PLA/EVA = 60:40 wt% to improve toughness while maintaining the biodegradability of the PLA. The polymers were first vacuum-dried overnight at 60°C before blending to eliminate water that should affect the processing and properties. Then, PLA and EVA were dry blended and introduced into the chamber of a Brabender plastograph equipped with a W50 EHT internal mixer (volume of 55 cm^3) and roller rotors at a temperature of 180°C and a rotating speed of 60 rpm. The total mixing time was 5 min. This time was enough to achieve the stable torque while decreasing the chance for the polymer degradation. For CNT modified with the IL mimbSO$_3$H·Cl (CNT/ILSO$_3$H), the pristine CNT (pCNT) was previously dispersed with IL in a proportion CNT/ILSO$_3$H = 1:2.5 and 1:5 wt/wt by grinding both components in a mortar for about 15 min. After that, the resulting CNT/ILSO$_3$H was blended with PLA and EVA using similar mixing protocol.

Before molding steps (injection or compression molding), the samples were milled and put in a vacuum oven at 60°C to dry the samples. The samples for mechanical and dynamic-mechanical analysis were injection molded in a Haake miniJet model, using the following parameters: barrel temperature = 180°C; injection pressure = 450 bar; mold temperature = 20°C; holding pressure: 250 bar, injection time: 10 s, holding time: 5 s. The total cycle time corresponded to 15 s. The samples for conductivity and rheological properties were compression-molded into disks of 20 mm diameter and 1 mm thickness in a hydraulic press at 180°C and pressure around 7 MPa for 3 min, followed by a cooling process at the same pressure using another hydraulic press at 20°C for 5 min.

CHARACTERIZATION

The molar mass of the PLA phase in the blends was determined by size exclusion chromatography (SEC) using a Shimadzu GPC, 803 equipped with 20A column (Column Phenomenex linear 300 × 7.8 mm, pore 5 μ) and a refractometer detector RID. Chloroform was used as eluent with a flow rate of 1 mL/min and at 22°C. The calibration curve was previously obtained with polystyrene standards in the range of 510–1,390,000 g/mol. For the SEC analysis, the PLA phase was extracted with chloroform, as follows: 2 g of the blend was stirred with 20 mL of chloroform during 48 h to extracted the PLA phase. Then, the solution was filtered and casting into Petri dish to evaporate the solvent at room temperature.

The rheological measurements were performed in a Discovery HR1 Hybrid rheometer from TA Instrument Inc., at 170°C, using parallel plate geometry (25 mm) with a distance of 1.0 mm between the plates. The measurements were performed in an oscillatory mode at a strain range from 0.1 to 100% under constant frequency of 1 Hz, which is within the linear viscoelastic regime. The testing temperature was fixed at 170°C to avoid excessive flow of the material out of the geometry and keep the fixed gap, since PLA used in this work has a high MFI and the testing cannot be performed at higher temperatures. This temperature was also employed in other studies involving PLA/EVA blends (Shi et al., 2013; Wang et al., 2016).

X-ray diffraction (XRD) measurements were performed on a Rigaku Ultima IV X-ray diffractometer (Cu Kα irradiation, 40 kV, 20 mA), in the range of 2θ from 1 to 40°.

Differential scanning calorimetry (DSC) of the blend and composites were performed on DSC Q20 from TA Instruments Inc. in dynamic mode under nitrogen flow of 50 mL·min^{-1}. The samples were submitted to the following protocol: first heating from 20 to 200°C at a rate of 10°C·min^{-1}; cooling up to 20°C at a rate of 10°C·min^{-1} and a second heating scan until 200°C at a rate of 10°C·min^{-1}.

Dynamic mechanical analysis (DMA) measurements were performed using a DMA Q800 TA Instruments at a fixed frequency of 1 Hz, strain of 0.1% and a heating rate of 3°C min^{-1}. The measurements were performed from −65 to 150°C, using single-cantilever clamp and rectangular samples with 17 × 12.7 × 3.2 mm dimensions, obtained by injection molding.

The morphology of the samples was observed through scanning electron microscopy (SEM) on a VEGA III from TESCAN operating at 15 kV. The injected samples were cryogenically fractured in liquid nitrogen and immersed into toluene at 50°C for 4 h to remove the EVA component. Then, the surface was washed with fresh toluene and alcohol with the aid of ultrasonic bath, according to the procedure reported by Bhattacharyya et al. (2005). The samples were dried and coated with gold for SEM examination.

The tensile properties were measured in a MTS Tytron 250 tensile tester at a crosshead speed of 5 mm·min^{-1}. The samples were injection molded into dimensions of the dumbbell-shaped tensile bars, according to the ASTM D-638-5 method.

The dielectric properties, including AC conductivity, were measured with an impedance analyzer Solartron SI 1260 gain phase analyzer equipped with a Solartron 1296 dielectric interface. The measurements were carried out at 25°C from 0.1 to 10^6 Hz with 0.1 V oscillating voltage with electrodes of 25 mm in diameter. The samples with 25 mm in diameter and 1 mm thickness were previously coated with a thin layer of gold in order to improve the contact.

RESULTS AND DISCUSSION

Rheological Behavior

The melt viscosity of the polymer components in a blend and the presence of filler exert strong influence on the rheological

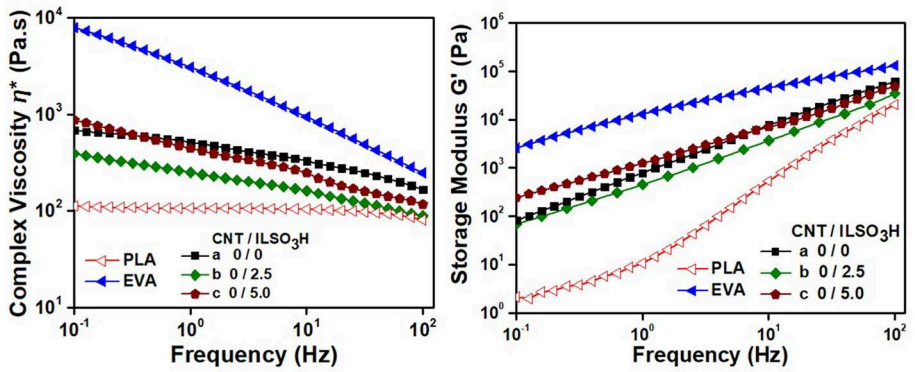

FIGURE 2 | Rheological parameters of PLA, EVA, and PLA/EVA blends loaded with CNT/$ILSO_3H$ in a proportion corresponding to (a) 0:0; (b) 0:2.5; and (c) 0:5.0 phr.

parameters and morphology of the final product. Therefore, it is important to investigate the effect of CNT and CNT/$ILSO_3H$ on the rheological parameters of the PLA/EVA blends. **Figures 2**, **3** illustrate the complex viscosity, η*, and storage modulus, G′, vs. frequency for the composites containing different proportions of IL or CNT/$ILSO_3H$, respectively. The rheological parameters of the pure components were also included for comparison. The η* and G′ values of PLA were significantly lower than those corresponding to the EVA component, mainly in the low frequency range. PLA also presented a Newtonian behavior at frequencies up to around 20 Hz, whereas EVA displayed a typical pseudo-plastic characteristic, with a significant decrease of η* as increasing the frequency. PLA grade with lower viscosity than EVA was chosen for this study to make easier the processability of the composites as the addition of CNT usually increases the melt viscosity of the system. Moreover, the lower viscosity of PLA associated with the higher proportion of this component ensures that this biodegradable polymer constitutes the matrix, which is interesting for biodegradability purpose.

The neat blend presented intermediary η* and G′ values and a less pseudo-plastic characteristic. The η* of the blend was lower than that reported by Li, et al. for PLA/EVA blends with PLA grade of higher molar mass, due to the lower molar mass of the PLA used in the present system (Li et al., 2011).

The presence of 2.5 phr of IL resulted in a decrease of η* and a slight decrease of G′, due to a plasticizing effect of the IL, a low molar compound. This plasticizing effect was also observed in the literature for other thermoplastic containing IL (Scott et al., 2002, 2003). However, an opposite effect was observed when the IL content was increased to 5 phr, that is, both η* and G′ increased when compared to the neat PLA/EVA blend. Moreover, a more pronounced pseudo-plastic behavior was observed for this mixture. This phenomenon may be related to the formation of graft copolymers between PLA and EVA through the transesterification reaction between the ester groups of both components promoted by IL that acts as a catalyst, as discussed in previous paper (Lopes Pereira et al., 2017). These reactions contribute for the compatibilization between the blend components. As the η* of EVA component is significantly higher than that of PLA, the EVA chemically attached to the PLA chains contributed for an increase of η* and G′, in spite of the presence of higher amount of IL, which usually acts as plasticizing. Also the interaction between IL and the blend component should contribute for an increase in viscosity, as stated by other authors (Yousfi et al., 2014).

The rheological parameters of the composites containing CNT modified with different amounts of IL are illustrated in **Figure 3**. The addition of 1 phr of CNT resulted in a significant increase of η* and G′ in the low frequency range. Moreover, the G′ vs. frequency slope at low frequencies decreased significantly. These features indicate that the CNT dispersed within the PLA/EVA matrix started to present a certain degree of interconnectivity, thus forming a physical networked structure. This characteristic was more pronounced for the composite loaded with CNT/$ILSO_3H$ in a proportion corresponding to 1:5. In this case, a more accentuated shear-thinning effect in the profile of the η* vs. frequency curve, as well as a higher G′ value at lower frequency range and a low G′ vs. frequency slope in the low frequency range were observed. All these features indicate that non-covalently functionalized CNT with the IL is more dispersed within the polymeric matrix, thus forming a more effective networked structure, which also was responsible for the higher electrical conductivity, as it will be discussed in the next sections. The IL at the surface of the CNT can favor the debundling of the aggregated hopes and bundles of CNT. This phenomenon was not so evident when lower amount of IL was employed. In fact, the composite containing CNT/$ILSO_3H$ (1:2.5) presented lower viscosity and G′ values than the composite containing only CNT, confirming the plasticizing/lubricating effect of this IL. The increase of melt viscosity with the addition of 1 wt% of CNT non-covalently functionalized with IL was also reported in our previous studies involving PP/PA12 blends (Lopes Pereira et al., 2019) or PP/PLA blends (Soares et al., 2019).

Morphology

Figure 4 illustrates the SEM micrographs of PLA/EVA (60:40 wt%) blend and the corresponding composites containing 1 phr of pristine CNT (pCNT) or CNT modified with IL (CNT/$ILSO_3H$). The images in the left side correspond to the micrographs obtained from non-etched surface samples and

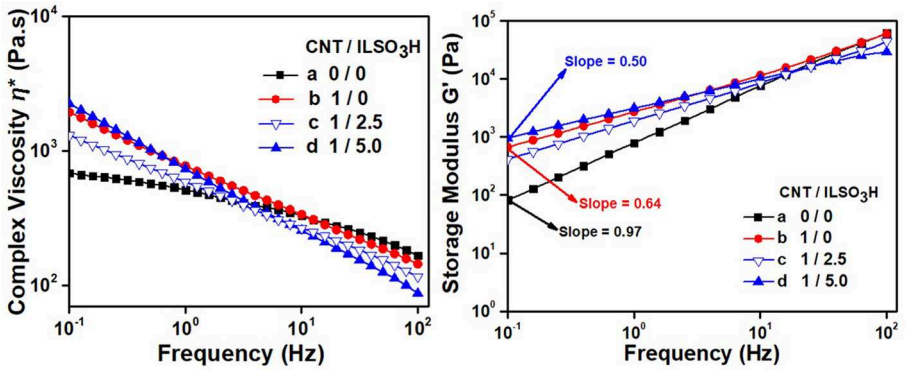

FIGURE 3 | Rheological parameters of PLA/EVA containing CNT/$ILSO_3H$ in a proportion of (a) 0:0; (b) 1:0; (c) 1:2.5; and (d) 1:5 phr.

those presented in the right side are related to the micrographs obtained from the etched surface samples in hot toluene. Then, the holes observed in these micrographs refer to the EVA phase that was removed after the treatment with toluene. The neat blend displayed a typical gross-separated and sea-island morphology with large EVA domains (**Figure 4a**). The extracted surface also presented large and non-homogeneous holes, confirming that the blend is incompatible/immiscible (**Figure 4a′**). The large domains were attributed to the great difference in viscosity between the blend components, being EVA much more viscous than PLA. When the viscosity of the dispersed phase is higher than the matrix, the morphology tends to present large domain size (Huang, 2011). The presence of pCNT exerted some influence on the blend morphology. Both non-extracted (**Figure 4b**) and extracted surface (**Figure 4b′**) displayed EVA domains with smaller size, as it was also observed in other heterogeneous blend loaded with CNT (Liebscher et al., 2013; Soares et al., 2018). The micrograph of the composite loaded with CNT/$ILSO_3H$ (1:5) also presented a more refined morphology. It is difficult to distinguish the EVA domains in the non-extracted surface (**Figure 4c**). However, it is possible to observe the presence of smaller holes formed from the extracted EVA phase (**Figure 4c′**). This behavior indicates that the IL at the CNT surface was able to improve the PLA/EVA compatibilization. The effect of IL on the morphology of the PLA/EVA blend is also presented in **Figures 4d,d′**. This blend also presents sea-island type morphology with relatively large EVA domains. However, the micrograph taken from non-etched surface suggests some kind of interfacial adhesion between matrix and dispersed phase, since the presence of cavities in the interface is not so evident. As discussed in our previous work (Lopes Pereira et al., 2017), the Bronsted acidic ionic liquid acts as catalyst for the transesterification between the ester groups of the EVA and PLA phase, enhancing the anchorage between them.

The changes in morphology of heterogeneous blends with the addition of CNT may be attributed to the increase of the shear forces due to the higher viscosity of the system imparted by the CNT and also some change in the viscosity ratio of the blend components, due to the preferential localization of CNT in one phase. According to thermodynamic calculation of the interfacial tension and wetting coefficient predicted in the literature, CNT presents a tendency to be located in the PLA phase (Shi et al., 2013). In our system, this should be also favored by the lower viscosity of the PLA phase. In order to estimate the localization of CNT, the CNT-loaded composites were submitted to a treatment with dichloromethane, which selectively extracted the PLA phase, and hot toluene, which extracts the EVA phase. After extraction, both chloroform and toluene appeared dark, indicating the presence of CNT in both phases. Although CNT has more affinity for the PLA phase as suggested by Shi et al. (2011) and also due to its lower viscosity, some amount of the filler was also located in EVA phase.

SEC Analysis

It was stated by several researchers in the literature that the transesterification reaction used for the reactive compatibilization of PLA-based blends may also provoke a decrease of the molar mass of the PLA phase due to the random cleavage of the ester groups along the PLA chain (Moura et al., 2012; Lins et al., 2015; Lopes Pereira et al., 2017). The magnitude of this phenomenon depends on the nature of the catalyst used during the reaction process. In our previous study, the use of 1 phr of the protonic ionic liquid, mimbSO_3H·Cl, as the catalyst for the compatibilization of PLA/EVA blend promoted a slight increase of the molar mass of the PLA phase, indicating that the degradation process was minimized by using this catalyst (Lopes Pereira et al., 2017). Therefore, the effect of the IL and CNT in different proportions on the molar mass of the PLA phase was investigated by SEC. **Table 1** summarizes the molar mass of PLA phase after submitting the blends to different treatment: mixing, mixing/injection molding and mixing/compression molding. The PLA extracted from the neat blend displayed significant decrease of the molar mass, when compared to the virgin PLA, indicating degradation process during the melt blending, as also observed in our previous study (Lopes Pereira et al., 2017) and by other authors (Park and Xanthos, 2009). The presence of EVA in the blend minimized the degradation process, since the molar mass of the PLA phase was higher than that of the neat

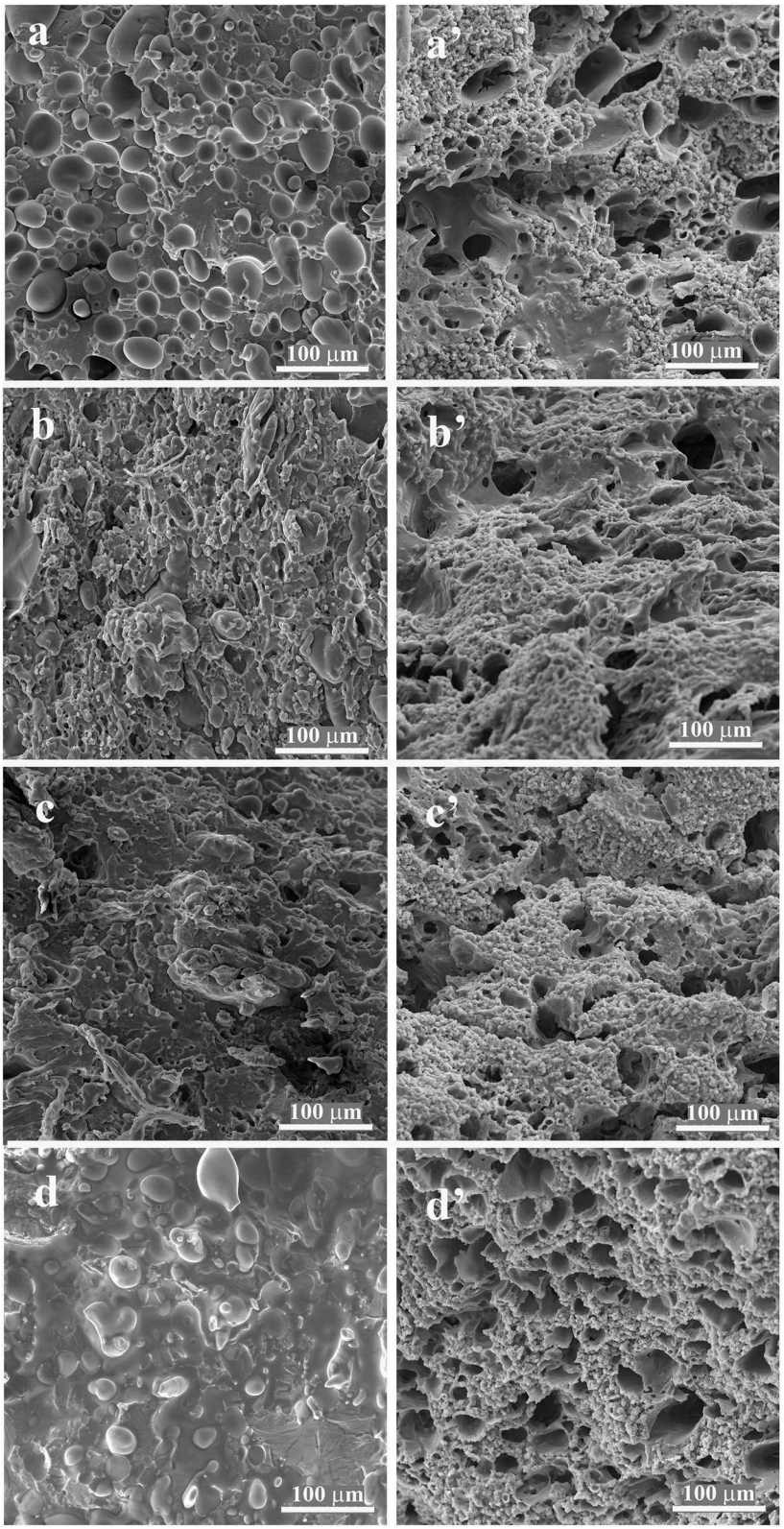

FIGURE 4 | SEM micrographs of non-etched surface of **(a)** PLA/EVA (60:40 wt%) blend and the composites containing **(b)** 1 phr of pCNT, **(c)** 6 phr of CNT/$ILSO_3H$ (1:5), and **(d)** 5 phr of $ILSO_3H$ (6 phr of CNT/$ILSO_3H$ corresponds to 1 phr of CNT in the system); and etched surface of the corresponding blend and composites **(a'-d')**.

TABLE 1 | Molar mass of PLA phase extracted from PLA/EVA (60:40 wt%) blends as a function of the processing conditions.

Filler content (phr)		Molar mass after mixing (Kg/mol)			Molar mass after mixing/injection molding (Kg/mol)			Molar mass after mixing/compression molding (Kg/mol)		
CNT	IL	Mw	Mn	PI	Mw	Mn	PI	Mw	Mn	PI
0[a]	0[a]	66	37	1.8	57	33	1.7	55	33	1.7
0	0	84	44	1.9	66	36	1.9	69	42	1.6
0	2.5	75	44	1.7	63	34	1.8	67	37	1.8
0	5.0	86	41	2.1	71	43	1.7	70	41	1.7
1	0	73	37	1.7	70	40	1.7	54	29	1.9
1	2.5	83	51	1.6	61	35	1.7	56	29	1.9
1	5.0	73	37	1.7	60	30	2.0	51	29	1.7

Unprocessed PLA; Mw = 124 Kg/mol; Mn = 80 Kg/mol; polydispersion index (PDI) = 1.5.

[a]*Values of neat PLA after processing.*

PLA after processing. The addition of the IL (2.5 phr) resulted in a decrease of Mw probably due to a cleavage of PLA chains promoted by the transesterification reaction. Increasing the amount of the IL (5 phr) resulted in a slight increase of Mw and a decrease of Mn. This behavior may be attributed to the transesterification reaction, which may occur between PLA and EVA chains or also between PLA chains. The last event should result in cleavage and combination of PLA chains. The presence of CNT promoted a degradation process of the PLA chains as indicated by a significant decrease of the molar mass. It is interesting to observe that the functionalization of CNT with the IL in a proportion CNT/ILSO_3H = 1:2.5 by mass promoted an increase of the PLA molar mass, when compared to the neat blend and that loaded with 1 phr of pCNT. This behavior suggests that the IL localized at the CNT surface minimized the deleterious degradation action of the CNT and helps on the compatibilization of the blend. Increasing the amount of IL to 5 phr resulted in a decreasing of the molar mass of PLA phase because the chain cleavage by transesterification reaction became more effective. The molding process also contributes for the degradation of PLA. In this context, PLA and the blends after submitting to the injection molding process resulted in additional decrease of MW, which may be explained by the high shear forces during the injection process. The molar mass of the blends without CNT did not present significant variation when submitted to injection or compression molding process. However, those loaded with CNT samples presented lower Mw and Mn values when submitted to compression molding when compared to those of the samples submitted to injection molding. This behavior may be attributed to the exposition of the samples to longer period at high temperature during the compression molding.

Crystallinity Behavior

The effect of CNT and CNT/ILSO_3H on the crystallinity behavior was investigated by X-ray diffraction (XRD) and DSC analysis. **Figure 5** presents the XRD patterns of PLA, EVA and the PLA/EVA blend and composites as a function of the processing parameters. Pure PLA submitted to compression molding process presented a broad amorphous halo over the entire 2θ range, indicating the amorphous nature of this sample. The injection molding induced some crystallinity to PLA, as the amorphous halo appeared together with a diffraction peak at $2\theta = 16.4^{\circ}$. This peak is related to the (200)/(110) plane of α-phase crystal of PLA (Zhang and Zhang, 2016). Pure EVA, both injection or compression molded, also presented an amorphous halo together with two diffraction peaks at $2\theta = 21$ and 23°, corresponding to the diffractions of (110) and (200) planes of EVA phase (Li et al., 2011). All PLA/EVA blend and composites displayed the characteristic diffraction peaks of the EVA component. However, no peak related to the PLA phase was observed, indicating that the PLA phase in the blend was completely amorphous regardless the processing conditions.

Differential scanning calorimetry (DSC) thermograms of PLA, EVA and their composites with EVA obtained during first heating scan and during the cooling process are illustrated in

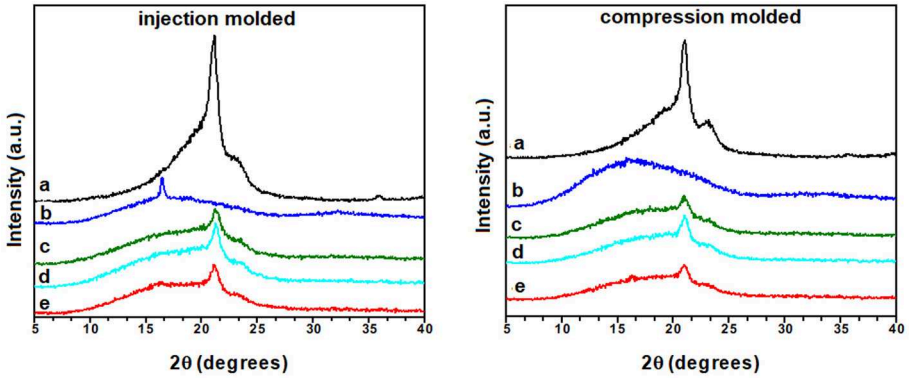

FIGURE 5 | XRD patterns of (a) EVA, (b) PLA, and the PLA/EVA (60:40 wt%) blends loaded with CNT/IL·SO_3H in the proportion of (c) 0:0; (d) 1:0; and (e) 1:5 phr.

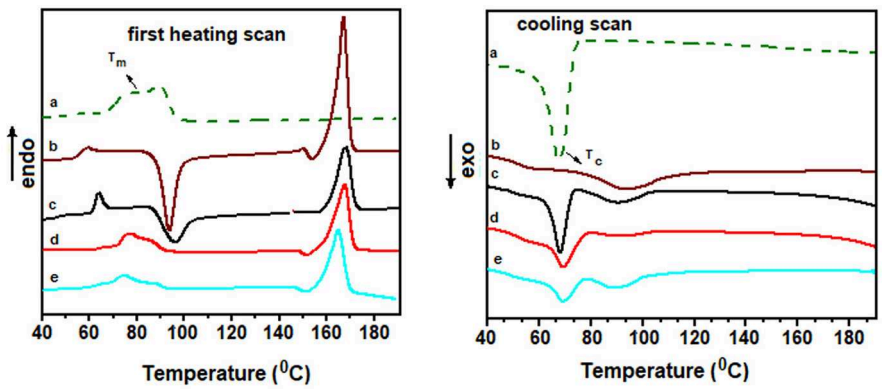

FIGURE 6 | First heating scan and cooling scan curves obtained from DSC thermograms of (a) EVA; (b) PLA; and the PLA/EVA (60:40 wt%) blends loaded with CNT/IL.SO_3H in the proportion of (c) 0:0; (d) 1:0; and (e) 1:5 phr.

Figure 6. The samples were obtained directly from the injection-molded specimens. **Table S1** presented in supplementary section summarizes the main data of the first and second heating scan, as well as, the cooling scan. Also **Figure S1** in the supplementary section illustrates the second heating scan curves. Pure PLA presented an endothermic transition at around 56°C, related to the glass transition temperature (T_g), an exothermic peak at around 94°C due to the cold crystallization temperature (T_{cc}) and an endothermic peak at around 167°C ascribed to the melting temperature (T_m). The prominent T_{cc} peak in the PLA sample is due to the slow crystallization process of PLA during processing. Pure EVA presented two broad endothermic peaks in the range of 76–90°C, which correspond to the T_m. This transition appeared close to the T_{cc} peak related to PLA. Blending with EVA did not exert great influence on the T_m of PLA, but resulted in a slight increase of T_{cc} from 94 to 97°C, suggesting that the EVA affected the crystallization process of PLA, as also found by other authors (Aghjeh et al., 2016; Agrawal et al., 2019). Nevertheless, by adding CNT of CNT/IL to the blend, the T_{cc} peak related to the PLA phase was suppressed, indicating that CNT and the CNT/IL exhibited great nucleating effect for the PLA crystallization, as also stated by other authors (Villmow et al., 2008).

The cooling scan curves presented clear exothermic peak at around 67–69°C, ascribed to the crystallization process of EVA component. The PLA phase displayed broad exothermic peak with very low intensity even for pure PLA sample, indicating slow crystallization process of PLA at this conditions. This feature is responsible for the appearance of the T_{cc} peaks in all blend and composites, during the second scan process (see **Figure S1** in the supplementary section). During the second scan, the presence of EVA did not affect the T_{cc} of PLA phase. However, the addition of CNT in the blend caused a slight increase of T_{cc}. Blend containing CNT/ILSO_3H = 1:5 presented a slight decreased of T_{cc} but a significant decrease of T_m, indicating that the CNT/IL system acts as nucleating agent favoring the crystallization of the PLA phase. This may be attributed to the interaction between IL and the PLA phase, which is increased due to the increase of the interfacial area due to the better CNT dispersion.

Mechanical and Dynamic-Mechanical Properties

Table 2 summarizes the tensile properties of PLA/EVA composites loaded with 1 phr of CNT modified with different IL proportions. The stress-strain curves are also illustrated in

TABLE 2 | Tensile properties of PLA/EVA (60:40 wt%) composites.

Filler content (phr)		Young modulus (MPa)	σ_B (MPa)	ϵ_B (%)
CNT	IL			
0[a]	0[a]	1,390 ± 55	41 ± 2.8	3.4 ± 0.7
0	0	690 ± 40	21 ± 3.0	9.0 ± 2.0
1.0	0	650 ± 30	21 ± 2.1	6.0 ± 0.5
1.0	2.5	660 ± 20	24 ± 3.0	8.0 ± 1.5
1.0	5.0	610 ± 25	21 ± 1.0	5.0 ± 0.3

[a] *Tensile properties of neat PLA; σ_B, tensile strength; ε_B, elongation at break.*

Figure S2 in supplementary section. PLA/EVA blend displayed a decrease of tensile strength and modulus when compared to neat PLA, but an increase of elongation at break (ϵ_B), due to flexible nature of EVA. The addition of pure CNT or that functionalized with IL did not exert significant influence on the tensile strength but decreased elongation at break. Similar behavior was also reported by Wang et al., for systems employing EVA50 and PLA/EVA with a composition of 80:20 (Wang et al., 2016). A slight improvement of ultimate tensile strength was observed when CNT/ILSO$_3$H (1:2.5) was used, probably due to some interfacial adhesion promoted by the compatibilization. In spite of some interfacial adhesion suggested by SEM micrograph and rheological measurements, the systems loaded with IL in higher proportion presented poorer mechanical properties. This behavior may be attributed to an increasing of a degradation process of PLA component through transesterification reaction involving ester groups in the middle of the PLA chain, as indicated by SEC analysis.

The dynamic mechanical properties of the composites are illustrated in **Figure 7** in terms of storage modulus (E′), loss factor (tan delta) and loss modulus (E″) as a function of the temperature. Also the main dynamic-mechanical parameters of the neat polymers are also summarized in **Table 3**. The storage modulus in the glassy region for the PLA/EVA blend increased with the addition of CNT, indicating a stiffness of the material due to the addition of the rigid filler. The composite loaded with CNT/ILSO$_3$H (1:2.5) resulted in an additional improvement of the modulus, probably due to a better dispersion of the CNT imparted by the presence of the IL at the surface. Increasing the amount of IL decreased the modulus when compared with those containing CNT probably due to a plasticizing effect of IL. These results suggest that the plasticizing effect of the low molar mass IL is effective in the solid state. In the melt state, as suggested by rheological measurements, the higher amount of IL resulted in an increase of the viscosity due to the better dispersion of the CNT and the formation of the physical networked structure. After around 50°C, E′ decreased due to the increase in chain mobility. The increase of the modulus at higher temperature is due to the cold crystallization phenomenon (Song et al., 2012; Agrawal et al., 2019). This characteristic is very common in PLA-based systems, due to its slow crystallization rate. The modulus in the rubbery region (at around 85°C) significantly increased for PLA/EVA blend when compared with the neat PLA. This phenomenon suggests that EVA exerts some reinforcing effect on

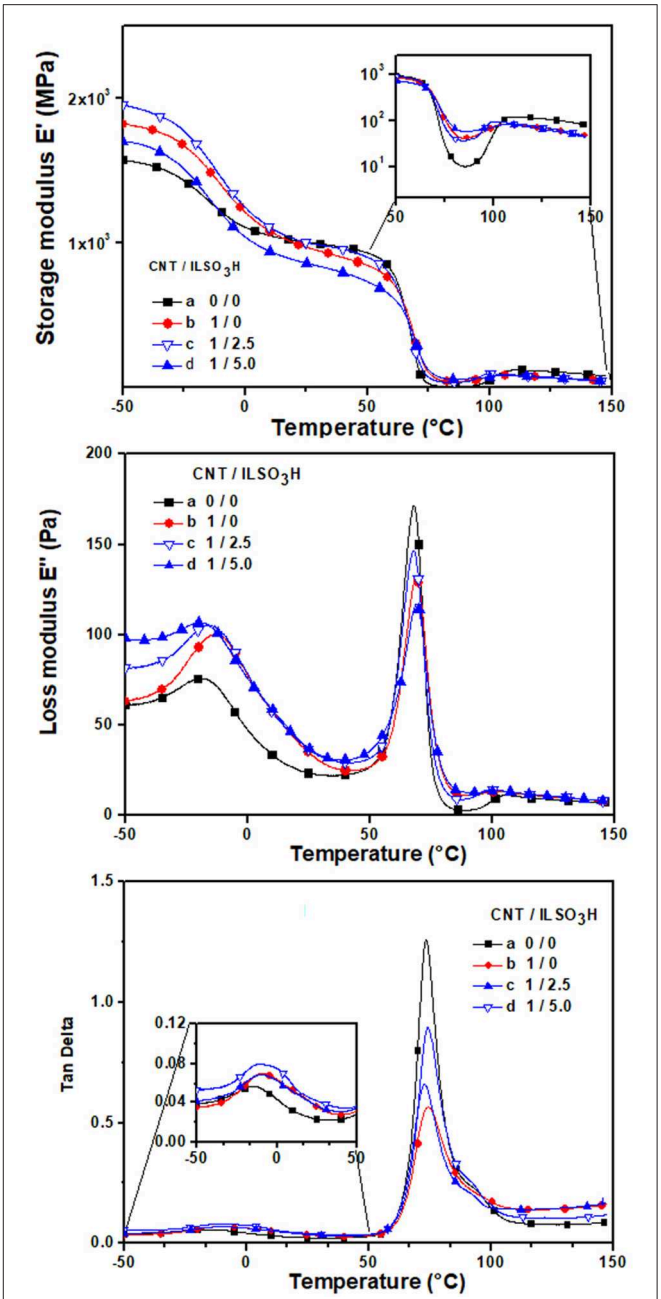

FIGURE 7 | Dynamic mechanical parameters as a function of the temperature for PLA/EVA blend containing CNT/ILSO$_3$H in a proportion of (a) 0:0; (b) 1:0; (c) 1:1.25; and (d) 1:5 phr.

the system probably due to an improvement of the crystallization process of PLA. The addition of CNT resulted in additional increase of E′ in the glassy region due to a reinforcing action of the filler. The use of CNT/ILSO$_3$H (1:2.5) also contributed for an additional increase of modulus, confirming the better dispersion state of the functionalized CNT with the IL and the formation of the networked structure in higher extent.

Another interesting feature observed in this region is the difference between the E′ values in the rubbery region and after

TABLE 3 | Dynamic mechanical properties of PLA, EVA, and PLA/EVA (60:40 wt%) composites.

Matrix (wt%)		Filler (phr)		E′ at −40°C (GPa)	E′ at 25°C (GPa)	E′ at 85°C (GPa)	Tg_{EVA} (°C)	Tg_{PLA} (°C)	I_{R-EVA}	I_{R-PLA}
PLA	EVA	CNT	IL							
100	0	0	0	2.1	2.0	0.005		69	–	–
0	100	0	0	1.7	0.1	–	−4		–	–
60	40	0	0	1.5	1.0	0.01	−14	73	0.29	5.73
60	40	1.0	0	1.8	1.0	0.04	−9	74	0.49	3.23
60	40	1.0	2.5	1.9	1.0	0.03	−9	73	0.40	2.98
60	40	1.0	5.0	1.7	0.9	0.06	−9	74	0.40	2.42

Tg from the maximum of Tan delta curves; I_R, integral area under the loss factor (tan delta).

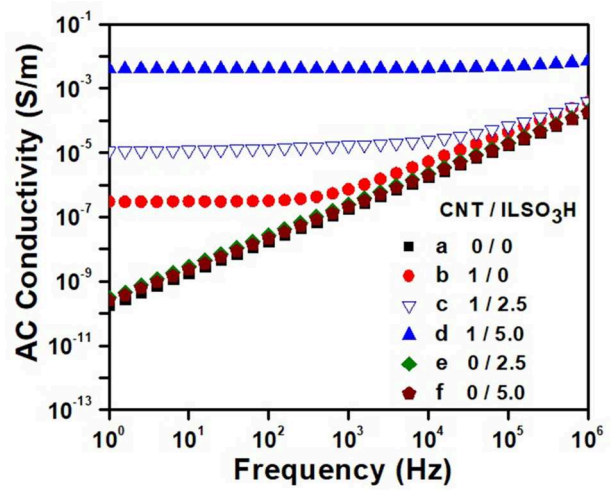

FIGURE 8 | AC electrical conductivity against frequency for PLA/EVA blends and composites containing CNT/$ILSO_3H$ in a proportion of (a) 0:0; (b) 1:0; (c) 1:1.25; (d) 1:5; (e) 0:2.5; and (f) 0:5.0 phr.

the cold crystallization phenomenon. This difference is smaller in the composite loaded with CNT than in neat polymer blend. This behavior may be related to the reinforcing action of CNT and also to the efficiency of CNT as nucleating agent, thus accelerating the crystallization process of PLA, as also reported in other studies Villmow et al. (2008). The presence of CNT/$ILSO_3H$ (1:5) decreased substantially this difference, that is, the cold crystallization phenomenon was almost absent, as observed from the DSC measurements during the first heating scan (see **Figure 6**). This behavior is also attributed to the better dispersion of CNT, thus increasing the interaction between the matrix and filler. Thus, the accelerating effect of the crystallization process was enhanced.

The effect of the CNT on the glass transition temperature of both PLA and EVA phases is also illustrated in **Figure 7** in terms of loss modulus and tan delta against temperature. The T_g values presented in **Table 3** were taken from the maximum of the tan delta curves. The T_g value of the EVA component in the blend is lower than that observed for the pure EVA, which may be attributed to an increase of the free volume at the interface due to the incompatibility between the blend component, as indicated by the SEM micrograph. The presence of CNT or CNT/IL did not exert significant influence on the T_g of the PLA phase, whose values stayed around 73–74°C. The Tg of the EVA phase slightly shifted toward higher temperature with the presence of CNT, which means a decreasing of the free volume in this phase. Moreover, some interaction between EVA phase and CNT may be responsible for this slight displacement of T_g. Similar features were also observed by Wang et al. (2016). According to the literature, the integral area (I_R) under the loss factor (tan delta) may be related to the total energy dissipated due to viscoelastic relaxation of the polymer chains (Jafari and Gupta, 2000; Wang et al., 2016). Thus, the I_R values can give an idea about the fracture toughness of polymers. **Table 3** presents the I_R values related to EVA and PLA relaxations in the composites. The presence of CNT in the blends resulted in higher I_{R-EVA} compared with neat blend. This behavior suggests an improvement of the toughness of the material (Wang et al., 2016). In the case of PLA component, the presence of CNT resulted in a decrease of the I_{R-PLA} values. This phenomenon may be related to an increase of stiffness of the PLA phase, caused by the presence of the rigid particle. It is interesting to point out that the non-covalent functionalization of CNT with ionic liquid promotes additional stiffness, indicated by lower I_R values for these samples. This result highlights the better dispersion of CNT promoted by the IL, thus forming a more effective physical network constituted by the dispersed CNT.

Electrical and Dielectric Properties

The dependence of the AC electrical conductivity with frequency for the PLA/EVA composites loaded with 1 phr CNT is illustrated in **Figure 8** as a function of the IL content. The blends containing only IL were also shown for comparison. The neat PLA/EVA blend and those containing only IL (2.5 or 5.0 phr—curves *e* and *f*) presented a linear dependence of the conductivity with the frequency, which is typical of insulating materials. The addition of 1 phr of pCNT (curve *b*) (without modification) resulted in composite with conductivity around 4×10^{-7} S/m in low frequency range and also a DC electrical conductivity plateau until a frequency of around 400 Hz. Beyond this frequency, known as critical frequency (f_c), the conductivity increased linearly with the frequency, obeying the Jonscher's universal power law for the frequency dependent conductivity of solids (Jonscher, 1977). This phenomenon arises from the presence of

trapped dipoles and charge carriers that cannot move at low frequencies but at higher frequencies, they have more chance to move due to the higher energy, thus displaying a typical non-ohmic conduction mechanism (frequency dependent) through tunneling/hopping effect (Min et al., 2013; Ram et al., 2017). Shi, et al. reached values around 10^{-5} S/m for PLA/EVA blend loaded with 1 wt% of CNT (Shi et al., 2013). However, it is difficult to compare the results as they used a master batch approach where CNT was previously dispersed in the PLA an also EVA component with 40% of vinyl acetate, whereas the processing conditions used in the present work involve only one processing step.

The functionalization of the CNT with the IL resulted in a significant increase of the conductivity. Moreover, the DC conductivity plateau is shifted toward higher frequency, indicating the formation of physical network of CNT in larger extent. The composite loaded with CNT/ILSO$_3$H (1:5) displayed conductivity value around 3.7×10^{-3} S/m (four order of magnitude higher than the blend containing pCNT) and frequency independent for all frequency range studied, characterizing a conductive material. Considering that no ionic conductivity was observed for the blends containing only IL, the outstanding electrical conductivity found for the composites containing CNT/ILSO$_3$H may be due to a better dispersion of the filler within the matrix imparted by the IL at the CNT surface. The IL contributes for a disaggregation of the CNT bundles and favors the formation of the conducting pathway in larger extent.

To investigate the effect of CNT and IL on the conduction mechanism that occurs in the PLA/EVA -based composites, the charge transport properties were estimated from the following power law equation (Jonscher, 1977):

$$\sigma_{AC} = \sigma_{DC} + k.f^n \quad (1)$$

where σ_{AC} is the AC electrical conductivity, σ_{DC} is the DC electrical conductivity, k is a constant dependent on temperature, f is the frequency and n is an exponent which provides an indication of the charge transport mechanism (Bose et al., 2008). The PLA/EVA composite loaded with 1 phr of CNT presented n value close to 0.96, indicating a charge transfer mechanism through hopping/tunneling, according to the literature (Bose et al., 2008). The composite loaded with CNT/ILSO$_3$H (1:2.5) displayed n value of 0.76, which characterizes a charge transfer mechanism through polarization effects, as stated by Bose et al. (2008). As also observed by Bose et al. (2008), the presence of IL facilitates the debundling of CNT and the contact between the conductive particles.

Table 4 compares the electrical conductivity of some thermoplastic matrices loaded with CNT/ionic liquid. As expected, the conductivity strongly depends on the nature of polymer matrix, nature and amount of IL used and processing conditions. However, it is possible to emphasize the significant increase in conductivity with the use of IL as dispersing agent for CNT. Some composites, including that reported in the present work, displayed an increase of conductivity by around four orders of magnitude.

Figure 9 shows the dependence of real permittivity (ϵ') and imaginary permittivity (ϵ'') of the composites with different CNT/ILSO$_3$H proportions with the frequency at room temperature. Both ϵ' and ϵ'' were independent of frequency in all measured frequency range, for the neat blend. The presence of pure IL (2.5 and 5.0 phr) did not significantly influence on the values of these properties and their dependence with frequency. Composite containing 1 phr of pCNT displayed very low ϵ' values but relatively high ϵ'' value, mainly in the low frequency range. This behavior suggests that the current leakage due to the movement of the mobile charge carrier throughout the materials is more important than the energy phenomenon storage.

The combination of CNT with the IL resulted in a significant increase of the ϵ' values for the corresponding composites, mainly in the low frequency region. The increase of ϵ' in the low frequency is related to the interfacial polarization, which usually occurs in heterogeneous systems with different dielectric constant, due to the accumulation of charge carriers at the interface between two materials (Jiang et al., 2009; Abraham et al., 2017). In this case, the ionic liquid at the CNT surface significantly contributes for the increasing of dielectric constant. This phenomenon cannot be only related to the contribution of the CNT and IL to the dielectric constant since these compounds, separately added to the blend, did not exert great influence on this

TABLE 4 | Electrical conductivity of heterogeneous polymer blends loaded with 1% of CNT-IL filler.

Matrix	Ionic liquid type	Conductivity (S/m)		References
		Without IL	With IL	
PMMA	Hmim·PF$_6$	10^{-9}	10^{-1}	Fang et al., 2018
PS	Alkyl-phosphonium-TFSI	10^{-4}	10^{-1}	Soares da Silva et al., 2017
PMMA	bmim·PF$_6$	10^{-11}	10^{-4}	Zhao et al., 2012
PC/PVDF	Aminopropyl-imidazol	10^{-5}	10^{-4}	Biswas et al., 2015
PVDF/ABS	Amino-terminated imidazol	10^{-3}	10^{-2}	Kar et al., 2015
PS/EVA	Alkyl-phosphonium-TFSI	5×10^{-1}	25×10^{-1}	Soares et al., 2018
PP/PA12	Alkyl-phosphonium-TFSI	3×10^{-7}	2×10^{-4}	Lopes Pereira et al., 2019
PP/PLA	Alkyl-phosphonium-TFSI	2×10^{-3}	10	Soares et al., 2019
PLA/EVA	mimbSO$_3$H·Cl	4×10^{-7}	3.7×10^{-3}	This work

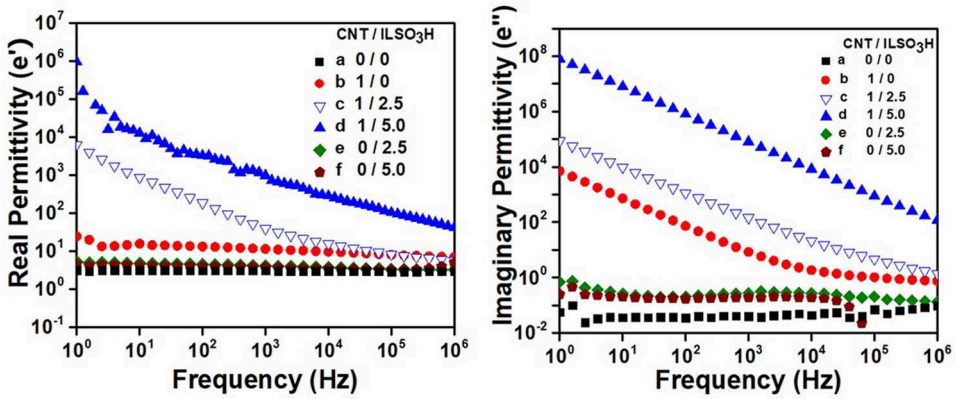

FIGURE 9 | Dielectric properties of PLA/EVA blends containing CNT/$ILSO_3H$ in a proportion of (a) 0:0; (b) 1:0; (c) 1:2.5; (d) 1:5; (e) 0:2.5; and (f) 0:5 phr.

property. In fact, the IL at the surface of CNT forms a thin layer between the polymer matrix and the filler that acts as numerous micro-capacitors. Increasing the amount of IL in these hybrid CNT/$ILSO_3H$ systems, increases the ϵ' values due to an increase of the interphase.

The imaginary permittivity (ϵ'') is mainly related to the energy dissipation within a dielectric. The increase of IL in the CNT/$ILSO_3H$ complex also resulted in a significant increase of ϵ'' of the corresponding PLA/EVA composites. This property is related to the conductivity and agrees with increased AC conductivity values found for these samples.

CONCLUSION

Conductive composites based on PLA/EVA loaded with CNT or CNT non-covalently functionalized with two different amounts of $mimbSO_3H{\cdot}Cl$ as the protonic ionic liquid were prepared by melt mixing. The presence of CNT/$ILSO_3H$ provided higher conductivity values to the composites when compared to that loaded with pristine CNT. The CNT/$ILSO_3H$ proportion corresponding to 1:5 by weight resulted in higher electrical conductivity, which was attributed to a better dispersion of CNT within the polymer matrix and the formation of a conducting pathway in larger extent. This feature was confirmed by rheological parameters in the melt state. Thus, higher viscosity and higher storage modulus were achieved using this CNT/$ILSO_3H$ proportion in the composite. Besides assisting the dispersion and debundling of the CNT during the melt processing, the IL also acted as interfacial agent between PLA and EVA phase, thus promoting a good interfacial adhesion. The compatibilization was suggested from SEM micrograph and also rheological properties. In fact, the presence of 5 phr of the $mimbSO_3H{\cdot}Cl$ resulted in an increase of the melt viscosity of the PLA/EVA blend. The results presented in this work highlight the dual effect of protonic ionic liquid as dispersing agent for CNT and also compatibilizing agent for PLA/EVA blends, and may considered a promising alternative for the development of semi-biodegradable conducting composites for antistatic packaging and other important applications in several fields of the electro-electronic industry.

DATA AVAILABILITY STATEMENT

All datasets generated for this study are included in the manuscript/**Supplementary Files**.

AUTHOR CONTRIBUTIONS

EL was responsible for the preparation of the samples and the management of their characterization. MS was responsible of the blends preparation and characterization. KP was involved in the main characterizations. BS was responsible for the general idea and was involved in the mains discussions of the results.

FUNDING

This work was sponsored in part by Coordenação de Aperfeiçoamento de Pessoal de Nível Superior–Brasil (CAPES)–(Grant number: 88887.333972/2019-00), Conselho Nacional de Desenvolvimento Científico e Tecnológico–CNPq (Grant number 303457/2013-9), and Fundação de Amparo à Pesquisa do Estado do Rio de Janeiro–FAPERJ (Grant number E-26/201.183/2014).

SUPPLEMENTARY MATERIAL

The Supplementary Material for this article can be found online at: https://www.frontiersin.org/articles/10.3389/fmats.2019.00234/full#supplementary-material

REFERENCES

Abraham, J., P, M. A., Xavier, P., Bose, S., George, S. C., Kalarikkal, N., et al. (2017). Investigation into dielectric behaviour and electromagnetic interference shielding effectiveness of conducting styrene butadiene rubber composites containing ionic liquid modified MWCNT. *Polymer* 112, 102–115. doi: 10.1016/j.polymer.2017.01.078

Aghjeh, M. R., Asadi, V., Mehdijabbar, P., Khonakdar, H. A., and Jafari, S. H. (2016). Application of linear rheology in determination of nanoclay localization in PLA/EVA/Clay nanocomposites: correlation with microstructure and thermal properties. *Compos. B Eng.* 86, 273–284. doi: 10.1016/j.compositesb.2015.09.064

Aghjeh, M. R., Nazari, M., Khonakdar, H. A., Jafari, S. H., Wagenknecht, U., and Heinrich, G. (2015). In depth analysis of micro-mechanism of mechanical property alternations in PLA/EVA/clay nanocomposites: a combined theoretical and experimental approach. *Mater. Des.* 88, 1277–1289. doi: 10.1016/j.matdes.2015.09.081

Agrawal, P., Araujo, A. P. M., Lima, J. C. C., Cavalcanti, S. N., Freitas, D. M. G., Farias, G. M. G., et al. (2019). Rheology, mechanical properties and morphology of poly(lactic acid)/ethylene vinyl acetate blends. *J. Polym. Environ*. 27, 1439–1448. doi: 10.1007/s10924-019-01445-8

Alves, F. F., Silva, A. A., and Soares, B. G. (2018). Epoxy—MWCNT composites prepared from master batch and powder dilution: effect of ionic liquid on dispersion and multifunctional properties. *Polym Eng. Sci*. 58:1689. doi: 10.1002/pen.24759

Bhattacharyya, A. R., Ghosh, A. K., Misra, A., and Eichhorn, K. J. (2005). Reactively compatibilized polyamide 6/ethylene-co-vinyl acetate blends: mechanical properties and morphology. *Polymer* 46, 1661–1674. doi: 10.1016/j.polymer.2004.12.012

Biswas, S., Kar, G. P., and Bose, S. (2015). Tailor-made distribution of nanoparticles in blend structure toward outstanding electromagnetic interference shielding. *ACS Appl. Mater. Interfaces* 7, 25448–25463. doi: 10.1021/acsami.5b08333

Bose, S., Bhattacharyya, A. R., Khare, R. A., Kulkarni, A. R., Patro, T. U., and Sivaraman, P. (2008). Tuning the dispersion of multiwall carbon nanotubes in co-continuous polymer blends: a generic approach. *Nanotechnology* 19:335704. doi: 10.1088/0957-4484/19/33/335704

Fang, D., Zhou, C., Liu, G; Luo, G., Gong, P., Yang, Q., et al. (2018). Effects of ionic liquids and thermal annealing on the rheological behavior and electrical properties of poly (methyl methacrylate)/carbon nanotubes composites. *Polymer* 148, 68–78. doi: 10.1016/j.polymer.2018.05.051

Fukushima, T., Kosaka, A., Ishimura, Y., Yamamoto, T., Takigawa, T., Ishii, N., et al. (2003). Molecular ordering of organic molten salts triggered by single-walled carbon nanotubes. *Science* 300, 2072–2074. doi: 10.1126/science.1082289

Hassouneh, S. S., Yu, L., Skov, L. A., and Daugaard., A. E. (2017). Soft and flexible conductive PDMS/MWCNT composites. *J Appl. Polym. Sci*. 134:44767. doi: 10.1002/app.44767

Huang, H. X. (2011). "Macro, micro and nanostructured morphologies of multiphase polymer systems," in *Chapter 6: Handbook of Multiphase Polymer, Systems, 1st Edn.*, eds A. Boudenne, L. Ibos, Y. Candau, and S. Thomas (John Wiley & Sons Ltd.), 161–249.

Jafari, S. H., and Gupta, A. H. (2000). Impact strength and dynamic mechanical properties correlation in elastomer-modified polypropylene. *J. Appl. Polym. Sci.* 78, 962–971. doi: 10.1002/1097-4628(20001031)78:5<962::AID-APP40>3.3.CO;2-X

Jiang, M. J., Dang, Z. M., Bozlar, M., Miomandre, F., and Bai, J. (2009). Broad-frequency dielectric behaviors in mulriwalled carbon nanotube/tuber nanocomposites. *J. Appl. Phys*. 106:084902. doi: 10.1063/1.3238306

Jonscher, A. K. (1977). The 'universal' dielectric response. *Nature* 267, 673–679. doi: 10.1038/267673a0

Kar, G. P., Biswas, S., Rohini, R., and Bose, S. (2015). Tailoring the dispersion of multiwall carbon nanotubes in co-continuous PVDF/ABS blends to design materials with enhanced electromagnetic interference shielding. *J. Mater. Chem. A* 3, 7974–7985. doi: 10.1039/C5TA01183C

Li, Y., Liu, L., Shi, Y., Xiang, F., Huang, T., Wang, Y., et al. (2011). Morphology, rheological, crystallization behavior and mechanical properties of poly (L-lactide)/ethylene-co-vinyl acetate blends with different VA contents. *J. Appl. Polym. Sci*. 121, 2688–2698. doi: 10.1002/app.33581

Liebscher, M., Tzounis, L., Pötschke, P., and Heinrich, G. (2013). Influence of the viscosity ratio in PC/SAN blends filled with MWCNTs on the morphological, electrical and melt rheological properties. *Polymer* 54, 6801–6808. doi: 10.1016/j.polymer.2013.10.040

Lim, L. T., Auras, R., and Rubino, M. (2008). Processing technology for poly(lactic acid). *Prog. Polymer Sci*. 33, 820–852. doi: 10.1016/j.progpolymsci.2008.05.004

Lins, L., Livi, S., Duchet-Rumeau, J., and Gerard, J. F. (2015). Phosphonium ionic liquids as new compatibilizing agents of biopolymer blends composed of poly(butylene-adipate-*co*-terephtalate)/poly(lactic acid) (PBAT/PLA). *RSC Adv*. 5:59082. doi: 10.1039/C5RA10241C

Liu, C. M., MA, F. F., Zhang, Z. X., Wang, Y., and Zhou, Z. W. (2016). Enhanced tensile creep stability of immiscible poly(L-lactide)/poly(ethylene vinyl acetate) blends achieved by adding carbon nanotubes. *Compos. B Eng.* 107, 174–181. doi: 10.1016/j.compositesb.2016.09.082

Lopes Pereira, E. C., Silva, J. M. F., Jesus, R. B., and Soares, B. G., Livi, S. (2017). Bronsted acidic ionic liquids: new transesterification agents for the compatibilization of polylactide/ethylene-co-vinyl acetate blends. *Eur. Polym. J.* 97, 104–111. doi: 10.1016/j.eurpolymj.2017.10.003

Lopes Pereira, E. C., Soares, B, G., Silva, A. A., Farias, S. J. M., Barra, G. M. O., Livi, S. (2019). Conductive heterogeneous blend composites of PP/PA12 filled with ionic liquids treated-CNT. *Polym. Test*. 74, 187–195. doi: 10.1016/j.polymertesting.2019.01.003

Lopes Pereira, E. C., and Soares, B. G. (2016). Conducting epoxy networks modified with non-covalently functionalized multi-walled carbon nanotube with imidazolium based–ionic liquid. *J. Appl. Polym. Sci*. 133:43976. doi: 10.1002/app.43976

Ma, P., Hristova-Bogaerds, D. G., Goossens, J. G. P., Spoelstra, A. B., Zhang, Y., Lemstra, P. J. (2012). Toughening of poly (lactic acid) by ethylene-co-vinyl acetate copolymer with different vinyl acetate contents. *Eur. Polym. J*. 48, 146–154. doi: 10.1016/j.eurpolymj.2011.10.015

Ma, P., Xu, P., Liu, W., Zhai, Y., Dong, W., Zhang, Y., et al. (2015). Bio-based poly(lactide)/ethylene-co-vinyl acetate thermoplastic vulcanizates by dynamic crosslinking: structure vs. property. *RSC Adv*. 5, 15962–15968. doi: 10.1039/C4RA14194F

Min, C., Yu, D., Cao, J., Wang, G., and Feng, L. (2013). A graphite nanoplatelet/epoxy composite with high dielectric constant and high thermal conductivity. *Carbon* 55, 116–125. doi: 10.1016/j.carbon.2012.12.017

Moura, I., Nogueira, R., Bournor-Legare, V., and Machado, A. V. (2011). Biobased grafted polyesters prepared by *in situ* ring-opening polymerization. *React. Funct. Polym.* 71, 694–703. doi: 10.1016/j.reactfunctpolym.2011.03.012

Moura, I., Nogueira, R., Bournor-Legare, V., and Machado, A. V. (2012). Synthesis of EVA-g-PLA copolymers using transesterification reactions. *Mater Chem. Phys*. 134, 103–110. doi: 10.1016/j.matchemphys.2012.02.036

Nampoothiri, K. M., Nair, N. R., and John, R. P. (2010). An overview of the recent developments in polylactide (PLA) research. *Bioresour. Technol*. 101, 8493–8501. doi: 10.1016/j.biortech.2010.05.092

Park, K. I., and Xanthos, M. (2009). A study on the degradation of polylactic acid in the presence of phosphonium ionic liquids. *Polym. Degrad. Stability* 94, 834–844. doi: 10.1016/j.polymdegradstab.2009.01.030

Ram, R., Rahaman, M., Aldalbahi, A., and Khastgir, D. (2017). Determination of percolation threshold and electrical conductivity of polyvinylidene fluoride (PVDF)/short carbon fiber (SCF) composites: effect of SCF aspect ratio. *Polym. Int*. 66, 573–582. doi: 10.1002/pi.5294

Sangeetha, V. H., Valapa, R. B., Nayak, S. K., and Varguese, T. O. (2016). Super toughened renewable poly (lactic acid) based ternary blends system: effect of degree of hydrolysis of ethylene vinyl acetate on impact and thermal properties. *RSC Adv*. 6, 72681–72691. doi: 10.1039/C6RA13366E

Sangeetha, V. H., Valapa, R. B., Nayak, S. K., and Varguese, T. O. (2018). Investigation on the influence of EVA content on the mechanical and thermal characteristics of poly(lactic acid) blends. *J. Polym. Environ.* 26, 1–14. doi: 10.1007/s10924-016-0906-0

Sarasa, J., Gracia, J. M., and Javierre, C. (2009). Study of the biodisintegration of a bioplastic material waste. *Bioresour. Technol*. 100, 3764–3768. doi: 10.1016/j.biortech.2008.11.049

Scott, M. P., Brazel, C. S., Benton, M. G., Mays, J. W., Holbrey, J. D., and Rogers, R. D. (2002). Application of ionic liquids as plasticizers for poly(methyl methacrylate). *Chem. Commun*. 13, 1370–1371. doi: 10.1039/b204316p

Scott, M. P., Rahman, M., and Brazel, C. S. (2003). Application of ionic liquids as low-volatility plasticizers for PMMA. *Eur. Polym. Sci.* 39, 1947–1953. doi: 10.1016/S0014-3057(03)00129-0

Shi, Y., Li, Y., Wu, J., Huang, T., Chen, C., Peng, Y., et al. (2011). Toughening of poly(L-lactide)/multiwalled carbon nanotubes nanocomposites with ethylene-co-vinyl acetate. *J. Polym. Sci. B Polym. Phys.* 49, 267–276. doi: 10.1002/polb.22177

Shi, Y., Li, Y., Xiang, F., Huang, T., Chen, C., Peng, Y., et al. (2012). Carbon nanotubes induced microstructure and mechanical properties changes in cocontinous poly(L-lactide)/ethylene-co-vinyl acetate blends. *Polym. Adv. Technol.* 23, 783–790. doi: 10.1002/pat.1959

Shi, Y. Y., Yang, J. H., Huang, T., Zhang, N., Chen, C., and Wang, Y. (2013). Selective localization of carbon nanotubes at the interface of poly(L-lactide)/ethylene-co-vinyl acetate resulting in lowered electrical resistivity. *Compos. B Eng.* 55, 463–469. doi: 10.1016/j.compositesb.2013.07.012

Soares da Silva, J. P., Soares, B. G., Livi, S., and Barra, G. M. O. (2017). Phosphonium–based ionic liquid as dispersing agent for MWCNT in melt-mixing polystyrene blends: rheology, electrical properties and EMI shielding effectiveness. *Mater Phys. Chem.* 189, 162–168. doi: 10.1016/j.matchemphys.2016.12.073

Soares, B. G. (2018). Ionic liquid: a smart approach for developing conducting polymer composites: a review. *J. Mol. Liquids* 262, 8–18. doi: 10.1016/j.molliq.2018.04.049

Soares, B. G., Calheiros, L. F., Silva, A. A., Indrusiak, T., Barra, G. M. O., and Livi, S. (2018). Conducting melt blending of polystyrene and EVA copolymer with carbon nanotube assisted by phosphonium-based ionic liquid. *J. Appl. Polym. Sci.* 135:45564. doi: 10.1002/app.45564

Soares, B. G., Cordeiro, E., Maia, J., Lopes Pereira, E. C., and Silva, A. A. (2019). The effect of the non-covalent functionalization of CNT by ionic liquid on electrical conductivity and electromagnetic interference shielding effectiveness of semi-biodegradable polypropylene/poly(lactic acid) composites. *Polym. Compos.* doi: 10.1002/pc.25347. [Epub ahead of print].

Song, P., Chen, G., Wei, Z., Chang, Y., Zhang, W., and Liang, J. (2012). Rapid crystallization of poly(l-lactic acid) induced by a nanoscaled zinc citrate complex as nucleating agent. *Polymer* 53, 4300–4309. doi: 10.1016/j.polymer.2012.07.032

Spitalsky, Z., Tasis, D., Papagelis, K., and Galiotis, C. (2010). Carbon nanotube-polymer composites: chemistry, processing, mechanical and electrical properties. *Prog. Polym. Sci.* 35, 357–401. doi: 10.1016/j.progpolymsci.2009.09.003

Subramaniam, K., Das, A., Simon, F., Heinrich, G. (2013). Networking of ionic liquid modified CNTs in SSBR. *Eur. Polym. J.* 49, 345–352. doi: 10.1016/j.eurpolymj.2012.10.023

Villmow, T., Pötschke, P., Pegel, S., Häussler, L., and Kretzschmar, B. (2008). Influence of twin-screw extrusion conditions on the dispersion of multi-walled carbon nanotubes in a poly (lactic acid) matrix. *Polymer* 49, 3500–3509. doi: 10.1016/j.polymer.2008.06.010

Wang, X., Zhang, Z., Li, J., Yang, J., Wang, Y., and Zhang, J. (2015). Largely improved fracture toughness of an immiscible poly(L-lactide)/ethylene-co-vinyl acetate blend achieved by adding carbon nanotubes. *RSC Adv.* 5, 69522–69533. doi: 10.1039/C5RA11192G

Wang, X. F., He, Z. Z., Yang, J. H., Zhang, N., Huang, T., Wang, Y., et al. (2016). Super toughened immiscible poly(L-lactide)/poly(ethylene vinyl acetate) (PLLA/EVA) blend achieved by *in situ* cross-linking reaction and carbon nanotubes. *Compos. A Appl. Sci. Manuf.* 91, 105–116. doi: 10.1016/j.compositesa.2016.09.020

Yamaki, S. B., Prado, E. A., and Atvars, T. D. Z. (2002). Phase transitions and relaxation processes in ethylene-vinyl acetate copolymers probed by fluorescence spectroscopy. *Eur. Polym. J.* 38, 1811–1826. doi: 10.1016/S0014-3057(02)00067-8

Yoon, J. S., Oh, S. H., Kim, M. N., Chin, I. J., and Kim, Y. H. (1999). Thermal and mechanical properties of poly (L-lactic acid)–poly (ethylene-co-vinyl acetate) blends. *Polymer* 40, 2303–2312. doi: 10.1016/S0032-3861(98)00463-7

Yousfi, M., Livi, S., and Duchet-Rumeau, J. (2014). Ionic liquids: a new way for the compatibilization of thermoplastic blends. *Chem. Eng. J.* 255, 513–524. doi: 10.1016/j.cej.2014.06.080

Zhang, N., and Lu, X. (2016). Morphology and properties of super-toughened bio-based poly(lactic acid)/poly(ethylene-co-vinyl acetate) blends by peroxide-induced dynamic vulcanization and interfacial compatibilization. *Polym. Test.* 56, 354–363. doi: 10.1016/j.polymertesting.2016.11.003

Zhang, X., and Zhang, Y. (2016). Reinforcement effect of poly(butylene succinate) (PBS)-grafted cellulose nanocrystal on toughened PBS/polylactic acid blends. *Carbohydr. Polym.* 140, 374–382. doi: 10.1016/j.carbpol.2015.12.073

Zhao, L., Li, Y., Cao, X., You, J., and Dong, W. (2012). Multifunctional role of an ionic liquid in melt-blended poly (methyl methacrylate)/multi-walled carbon nanotube nanocomposites. *Nanotechnology* 23:255702. doi: 10.1088/0957-4484/23/25/255702

Conflict of Interest: The authors declare that the research was conducted in the absence of any commercial or financial relationships that could be construed as a potential conflict of interest.